ISBN: 978-3-95450-204-2 ISSN: 2673-5350 doi:10.18429/JACoW-IBIC2019-MOBO02

BEAM INSTRUMENTATION AT THE FERMILAB IOTA RING*

N. Eddy†, D. R. Broemmelsiek, K. Carlson, D. J. Crawford, J. Diamond, D. R. Edstrom, B. Fellenz, M. A. Ibrahim, J. Jarvis, V. Lebedev, S. Nagaitsev, J. Ruan, J. K. Santucci, A. Semenov, V. Shiltsev, G. Stancari, A. Valishev, D. Voy, A. Warner, Fermilab, Illinois, USA
N. Kuklev, I. Lobach, University of Chicago, Illinois, USA
S. Szustkowski, Northern Illinois University, Illinois, USA

Abstract

The Integrable Optics Test Accelerator (IOTA) is a storage ring located at the end of the Fermilab Accelerator Science and Technology (FAST) facility. The complex is intended to support accelerator R&D for the next generation of particle accelerators. The IOTA ring is currently operating with 100 MeV electrons injected from the FAST Linac and will also receive 2.5 MeV protons from the IOTA Proton Injector currently being installed. The current instrumentation and results from the first electron commissioning run will be presented along with future plans.

INTRODUCTION

The Integrable Optics Test Accelerator (IOTA) is a storage ring which is a component of the Fermilab Accelerator Science and Technology (FAST) facility. The facility is dedicated entirely to research and development for the next generation of particle accelerators. IOTA is a storage ring with a circumference of 40 meters which can store beams at momenta between 50 and 200 MeV/c. The main goals for IOTA are to demonstrate the advantages of nonlinear integrable lattices [1,2] for high intensity particle beams and to demonstrate new beam cooling methods [3].

FAST has begun operations with electron beam from the super-conducting linear accelerator [4]. The electron linac provides a lot of flexibility to adjust the energy and intensity of the injected electron beam to match the beam envelope within the IOTA ring for commissioning as well as different experimental setups. The key features are the electron gun, capture cavities, and super-conducting Tesla style cryomodule with eight accelerating cavities.

Once injected into IOTA, the electron beam is cooled by synchrotron radiation to very low emittance. This allows a wider range of diagnostics tools which provide more accurate measurements than are possible with the proton beams. The electron beam operation is critical for precision understanding of the IOTA lattice and operations with the key focus being nonlinear integrable optics and optical stochastic cooling.

The layout of the ring is shown in Figure 1. The main design parameters for the IOTA ring are shown in Table 1. Some of the key elements are a dual frequency Radio Frequency (RF) accelerating cavity, horizontal and vertical strip-line kickers, 8 bend dipoles each with a horizontal trim, 39 quadrupole magnets powered in pairs, and 20 skew-quadrupole magnets each with horizontal and vertical trim magnets.

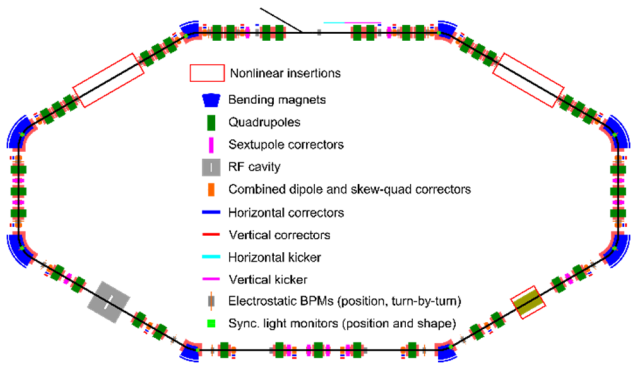

Figure 1: The layout of the IOTA ring.

Table 1: IOTA Design Parameters

Parameter	Value
Ring Circumference	39.97 m
Momentum Acceptance	50-200 MeV/c
Electrons	150 MeV/c
Protons	70 MeV/c
RF Frequency (electrons)	30.034 MHz
RF Frequency (protons)	2.19 MHz
RF Voltage	1 kV
Harmonic Number	4
Bunch Length (electrons)	10-20 cm
Tune (horizontal, vertical)	5.3, 5.3
Synchrotron Frequency	43 kHz

BEAM INSTRUMENTATION

The IOTA ring is equipped with a Direct Current Current Transformer (DCCT), 8 Synchrotron Light Monitor stations, 21 Beam Position Monitors (BPM), and a resistive Wall Current Monitor (WCM). In the course of the first run both a longitudinal and a transverse feedback system were also implemented.

DCCT Intensity Monitor

The IOTA DCCT is a Bergoz MPCT-RH-113 model, which was purchased for Booster R&D project in 1999. It was never used operationally and removed from the beamline in 2016. When the unit was retrieved, the signal cable was damaged from radiation a few inches from the sensor head. Unlike the new MPCT, the cable came right out of the sensor without a DB connector on that end. An attempt was made to repair the cable, but it turned out the wires

* Work supported by Fermi Research Alliance, LLC under Contract No. DE-AC02-07CH11359 with the U.S. Department of Energy, Office of Science, Office of High Energy Physics.
† eddy@fnal.gov

ISBN: 978-3-95450-204-2 ISSN: 2673-5350 doi:10.18429/JACoW-IBIC2019-MOBO02

inside were also damaged. The unit only worked intermittently. Bergoz assembled a new MPCT-S-113 sensor, which was calibrated and tested to match it to the original MPCT Electronics. The unit as installed into IOTA in 2018. The specifications for the MPCT are shown in Table 2.

Table 2: MPCT Specifications

Parameter	Value
Resolution	10μA rms
Linearity Error	< 0.1% Full Scale
Ripple RMS	< 0.2% Full Scale
Bandwidth	DC to 4.2 kHz

The MPCT signal is amplified and conditioned with an analog low pass filter and notch filter. The signal is then sampled at 10KHz. A 15Hz average signal is also provided by averaging within the control system. During commissioning, the signal was dominated by 720Hz. Investigations discovered that it was largely due to coupling to a nearby 3/4" Heliax cable, which connects the RF cavity probe to the ESB service building as shown in Figure 2. The noise was abated after a cable was ran to tie Earth Ground to both the tunnel and the racks.

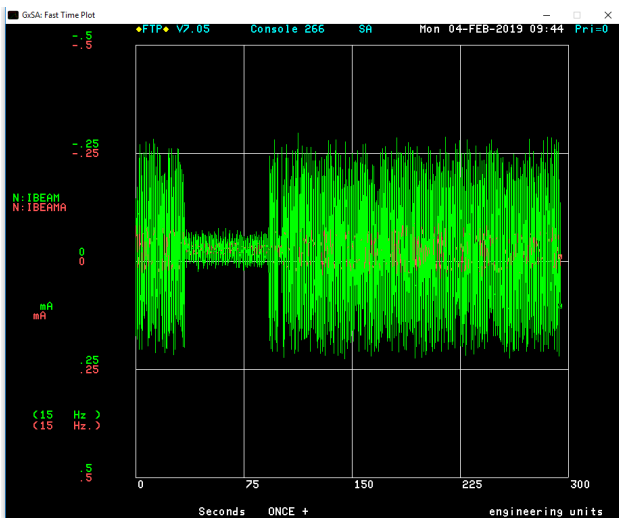

Figure 2: Noise on the DCCT readback with the RF probe connected and disconnected.

Synchrotron Light Monitors

Each of the eight bending dipoles is instrumented with a Synchrotron Light Monitor station further referred to as SyncLight. The SyncLight system is a powerful diagnostic which can provide transverse beam profiles, emittance, as well as beam position and intensity [5]. There are four dipole magnets with 60° bends and four with 30° bends with optically transparent windows downstream so that the Synchrotron Radiation (SR) can be extracted. In the base configuration, each station has a periscope transport line and a modular detection station situated on top of the magnet. Each station is outfitted with a low-noise CMOS camera, and can also be configured with photomultiplier tubes (PMTs), color wheels, polarizers, and other devices. It also contains various support electronics such as a Raspberry PI motor control and fanouts for add-on connectivity including power and ethernet.

All the key components within each station are motorized, allowing for remote alignment and changes to the optical configuration. The main camera detector is read out at 10FPS to an external DAQ server cluster which processes the images in real time to extract beam size, position, and intensity. This information is then compressed and made available to user consoles and the general accelerator controls network. A typical SyncLight station configuration is shown in Figure 3.

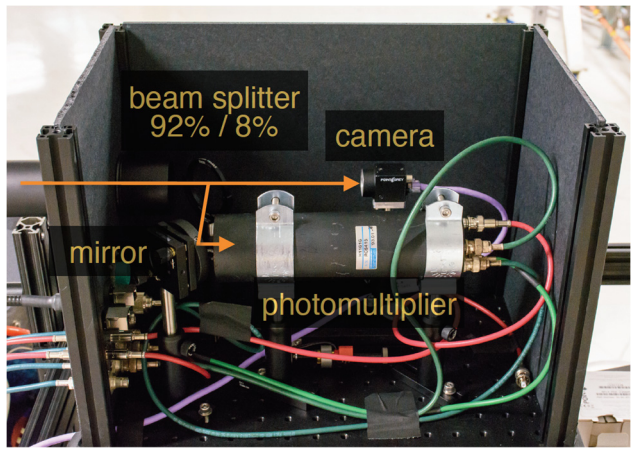

Figure 3: A typical SyncLight station configuration.

Beam Position Monitors

Beam Position Monitor (BPM) system was central to commissioning the IOTA ring as well as a number of experimental programs. There are 21 electrostatic button BPMs installed in the ring. Each pickup has four button electrodes with 20 pickups located symmetrically about the ring and one special large aperture pickup located in the injection region. Each BPM provides horizontal and vertical position as well as intensity. The BPM system consists of analog signal conditioning electronics, custom digitizer and DSP module, and a real-time Linux based front-end controller as shown in Figure 4.

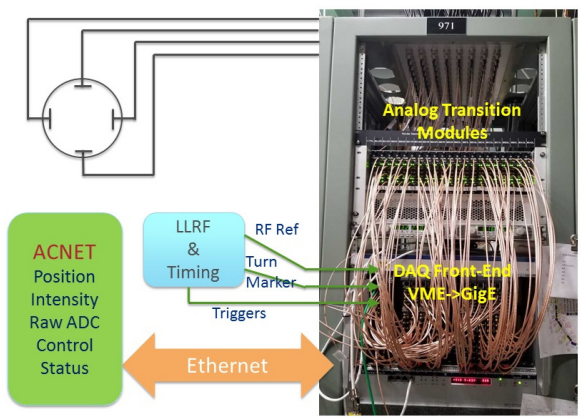

Figure 4: The BPM system layout.

The analog modules provide filtering, signal conditioning, and 32 db of programmable gain control as shown in Figure 5. The system was modified for IOTA to use an RF

ISBN: 978-3-95450-204-2 ISSN: 2673-5350 doi:10.18429/JACoW-IBIC2019-MOBO02

envelope detector instead of a band-pass filter to provide a clean bunch by bunch signal. The signals are then digitized and processed in the custom 8 channel digitizer modules shown in Figure 6. In the initial configuration, the signal for each bunch was integrated to provide the electrode magnitude for each bunch. The front-end controller reads out the processed magnitudes from the digitizers and calculates transverse positions and intensity for each bunch. The positions were calculated by doing a 2D polynomial fit calculated from the pickup mapping and the intensity as the sum of the magnitudes. The data was then provided to users and the accelerator control system as turn by turn array data for each bunch on request.

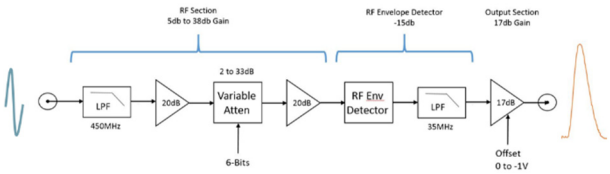

Figure 5: A block diagram of the BPM analog transition module showing the few ns input doublet from the button and the resulting output pulse.

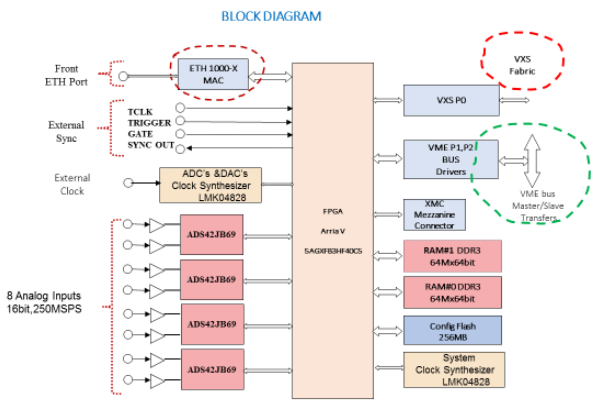

Figure 6: Custom 8 channel 16 bit 250 MS/s digitizer developed at Fermilab. The module is VME/VXS/GigE capable.

The system based upon the RF detector suffered from the fact that it was sensitive to both the bunch intensity and bunch length. This was a major issue for first commissioning and greatly impacted the system performance when the stored beam was below the design specifications for intensity and bunch length. The system was modified extensively to provide usable data to tune the machine during startup with lower than expected beam signals. This included adding 32 db RF amplifiers directly at the pickup at the tunnel to critical BPMs and numerous changes to the signal processing algorithms in the digitizers including peak and baseline measurements on each bunch, averaging up to 255 turns for each bunch, and finally implementing a linear fit algorithm to the difference over sum [6]. This also removed the need for a baseline calculation and allowed the digitizer inputs to be switched from DC coupled to AC coupled. Unfortunately, the averaging and orbit measurements made clear another issue with the system which was linearity with the RF detectors particularly for very small signals illustrated in Figure 7. The biggest benefit to the bpm system during the first run was the implementation of the longitudinal feedback system for the RF.

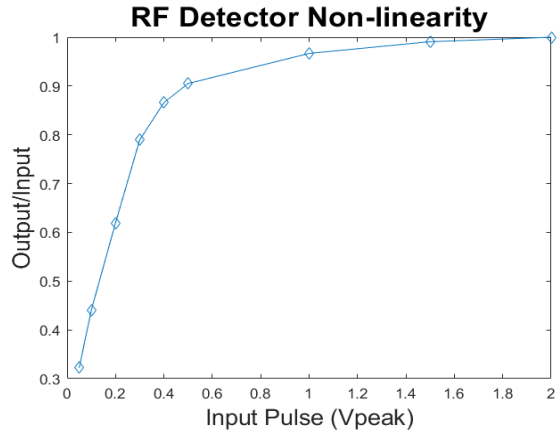

Figure 7: The ratio of the input to output from the RF detector as a function of the input pulse amplitude.

Wall Current Monitor

A high bandwidth Wall Current Monitor (WCM) was installed to provide high bandwidth longitudinal diagnostics. The Fermilab design was first developed for the EMMA ring at the STFC Daresbury Laboratory in the UK [7]. The lower frequency limit of the WCM is about 16KHz and is determined by the gap resistance and the ferrite inductance. The upper frequency is limited to about 4 GHz by the microwave cut-off frequency of the higher order modes. The measured response is shown in Figure 8. The device provides better than 0.5º phase resolution at the 30 MHz RF used in IOTA. The WCM proved to be critical in identifying the RF instabilities and implementing the longitudinal feedback system.

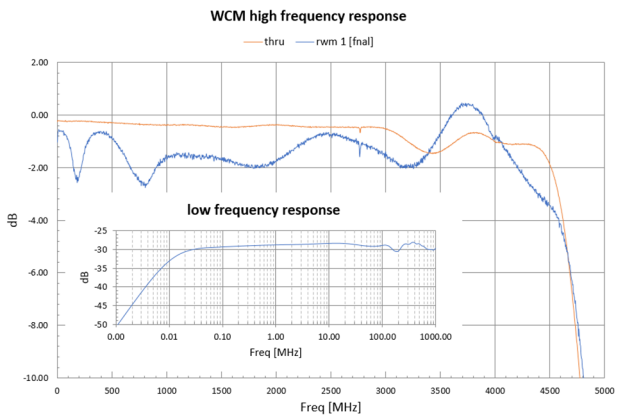

Figure 8: Measured WCM frequency response.

Longitudinal Feedback System

During commissioning it was found that longitudinal instabilities driven by high-order modes were limiting intensity in the machine and causing poor life-time as well as limiting the performance of other systems such as the BPMs. Looking at the wall current monitor data clearly showed large oscillations and instabilities occurring frequently. An effort was begun to design and implement a

ISBN: 978-3-95450-204-2 ISSN: 2673-5350 doi:10.18429/JACoW-IBIC2019-MOB002

longitudinal feedback system for the RF drive as shown in Figure 9. Once the system became operational it became possible to store beam at currents up to 4.5 mA which is almost 4 times higher than the design current of 1.2 mA. The longitudinal damper had a significant positive impact on commissioning as well as the experimental program.

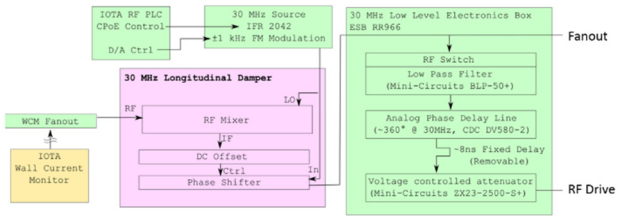

Figure 9: A block diagram of the low level RF system with the longitudinal damper implemented. The IF out of the mixer is limited to 10kHz.

Transverse Feedback System

A transverse feedback system was also designed and implemented with the goal to mimic beam instabilities rather than suppress them. A block diagram of the system is shown in Figure 10. The system made use of one of the horizontal kicker plates (the other being used for studies) and a BPM. The BPM was chosen to provide approximately 90° phase advance from pickup to kicker based upon cable delays and a list of non-critical bpm candidates. The total delay from pickup to kicker was just under 5 turns. The system was phased in by adjusting cable delays to align the resulting kick with the beam signal on the kicker fan-back monitor. Figure 11 shows the open loop system response after the system was phased in.

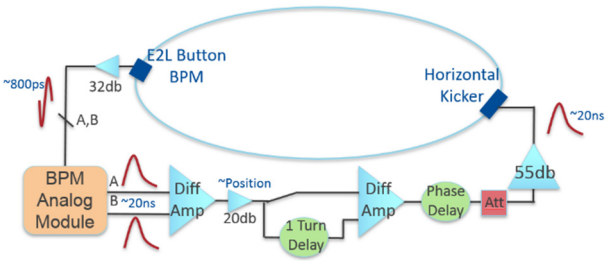

Figure 10: The transverse feedback system.

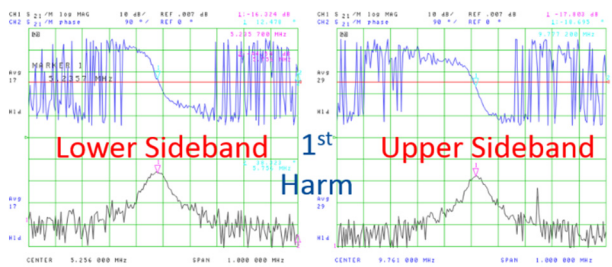

Figure 11: The open loop system response around the 1st revolution harmonic after phasing in.

COMMISSIONING AND FIRST RUN

The start of the first IOTA run highlights the flexibility of the facility. Due to issues with the linac cryomodule and the accelerating RF cavity in IOTA, a plan was developed to begin commissioning with electron beams with a momentum of 47 MeV/c using only the capture cavities in the linac and without the RF cavity in the ring. In this mode, it was possible to verify operation and control of key subsystems while demonstrating stored electron beam within the IOTA ring. In June of 2018, the BPMs were used to provide first turn information to get beam around the ring and eventually provide up to 200 turns of data before the beam decoherence caused the signals to fall into the noise. Before shutting down in August 2018, the WCM was able to see the beam for about 7500 turns (1 ms) while the DCCT was able to see a signal for 300000 turns (40 ms) before the beam was lost due to synchrotron radiation as shown in Figure 12. The SyncLight monitors were not available during this run.

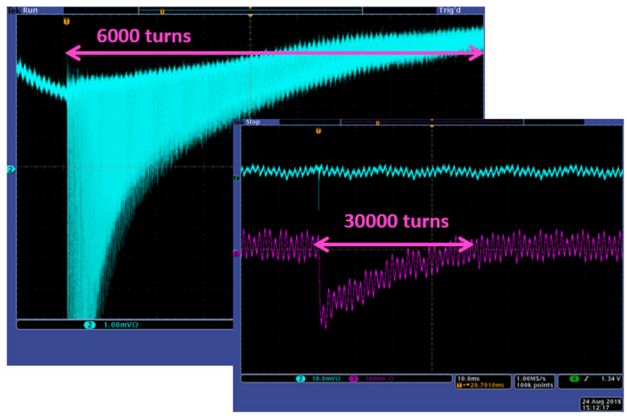

Figure 12: The WCM (cyan) and DCCT (pink) signals for stored beam after tuning with no ring RF on 1ms and 100ms scales.

After a short shutdown to fix the linac issues and install the RF cavity in the IOTA ring, the run continued with injection of electron beam at a momentum of 100 MeV/c. Commissioning and operations began in earnest over the next several months which entailed detailed checkout of all systems (electrical and mechanical), RF, timing, and diagnostics for proper function and to understand system performance.

First beam capture by the RF was achieved in October of 2018. By November of 2018, all 8 SyncLight stations were installed and began to provide high resolution orbit information. This provided a boost to the optics and lattice tuning which were struggling at the time due to poor resolution due to intensity and structure of the stored beam which was resulting in signals from the BPM pickups an order of magnitude below expectations from the design parameters.

Continuous efforts throughout the run were directed towards improving the precision of the turn-by-turn coordinate data returned by the BPM. Because of extremely small signals early in the run, numerous changes were made to improve the signal to noise of the system. The 32 db RF amplifiers in the tunnel provided usable turn-by-turn for the small signals as shown in Figure 13, but only a handful of bpms could be equipped. While small gains were made, the biggest improvement on the signal to noise

ISBN: 978-3-95450-204-2 ISSN: 2673-5350 doi:10.18429/JACoW-IBIC2019-MOBO02

occurred with the implementation of the longitudinal damper. Figure 14 shows turn-by-turn data taken at the end of the run with no pre-amps installed. Quality of life improvements were also made in the timing module to generate a serial trigger to each digitizer that was synchronized with the RF and encoded the type of data to collect. This alleviated the need to re-time the system when external changes were made to the RF system during commissioning.

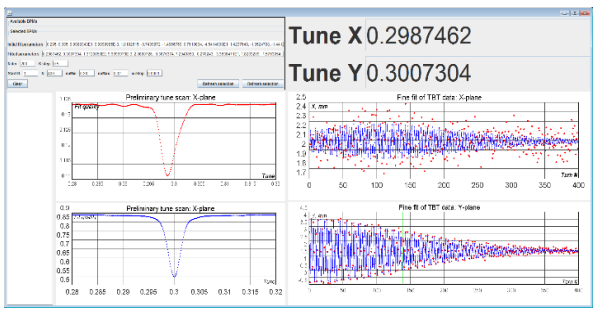

Figure 13: BPM TBT data and tunes taken on the nominal orbit with RF pre-amps in December 2018.

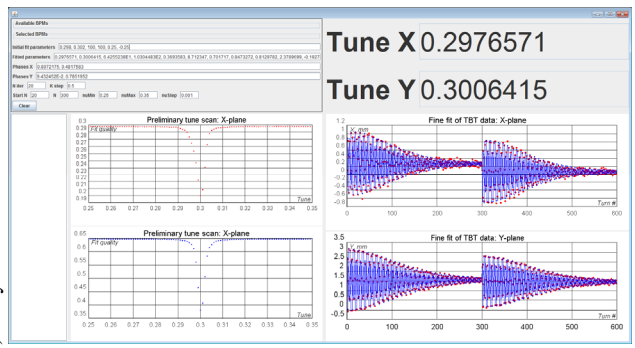

Figure 14: BPM TBT data and tunes taken on the nominal orbit with RF pre-amps removed and longitudinal damper installed in March 2019.

The SyncLight system was used extensively throughout the run. As a position monitor it had very good orbit resolution and linearity which provided some of the best constraints for orbit based lattice measurements due to non-linearity issues with the BPMs. The performance of the system was improved continuously throughout the run to improve system magnification and intensity calibrations. Short term measurements showed position resolution on the 100 nm scale for near gaussian beams which was several orders of magnitude lower than the observed orbit drifts. A live display of the SyncLight monitors is shown in Figure 15.

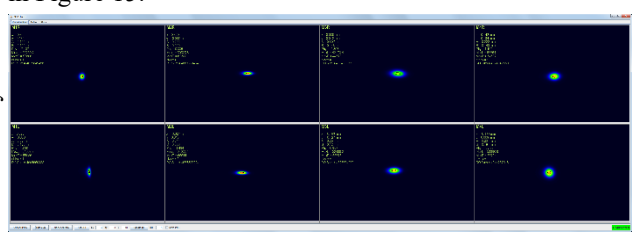

Figure 15: SyncLight system live display.

Once the BPM system began working as expected and the SyncLight systems were all operational, quick progress was made on the lattice and experiments began with studying the improvements non-linear beam dynamics [8]. Two of the highlights from the run were measurements of a single electron done using the SyncLight system shown in Figure 16 and the improved transverse stability with octupoles observed in Figure 17. Nearly twice the feedback gain is needed to induce an instability due to improved Landau damping from the octupoles.

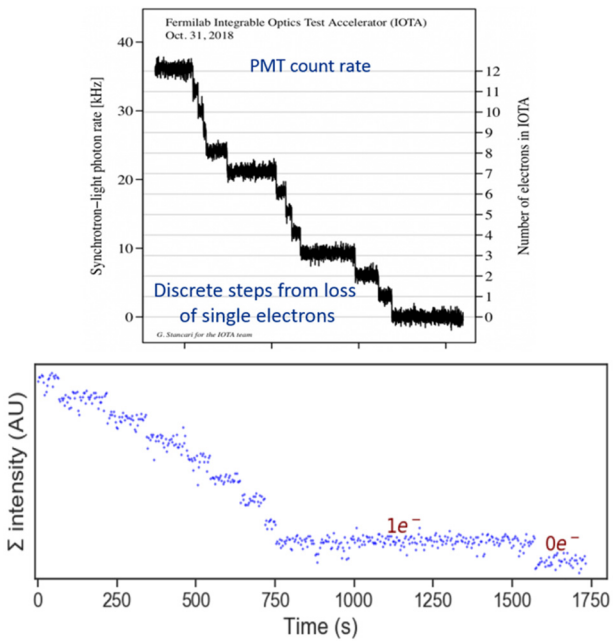

Figure 16: Single electron detection from PMT counting rates (top) and from sum pixel intensities from a single camera (bottom).

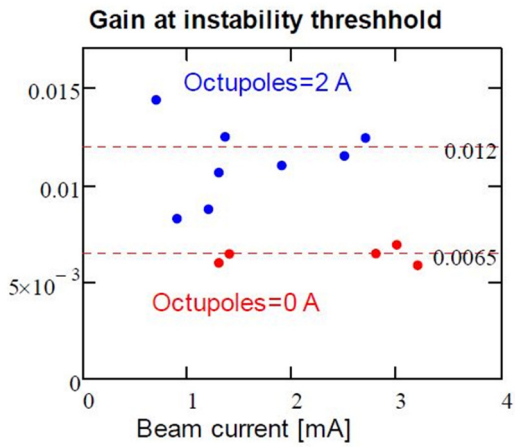

Figure 17: Improved Landau Damping with Octupoles.

FUTURE UPGRADES

BPM Upgrades

The main upgrade for the BPM system is to add high impedance pre-amplifiers to the pickups in the tunnel and

ISBN: 978-3-95450-204-2 ISSN: 2673-5350 doi:10.18429/JACoW-IBIC2019-MOBO02

remove the RF envelope detectors. This will solve the linearity issues as well as make the system resolution insensitive to bunch length. The frequency response of the button pickup with the new pre-amplifier is shown in Figure 18 with the inset showing a block diagram of the the pre-amplifier circuit. This solution also has the advantage that it will work for proton beam as well by amplifying the 30 MHz modulation which will be put on the beam. The digitizer readout is being switched from VME to a GigE interface which will provide a factor of 10 improvement to readout speeds and also allow the replacement of the front-end controller with a rack mount server which will greatly improve the acquisition of large data sets for users.

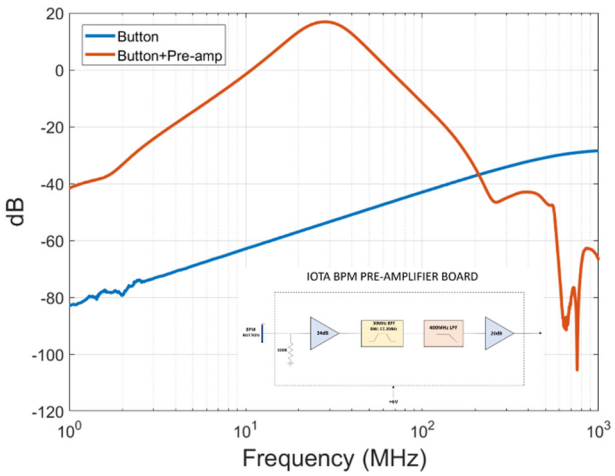

Figure 18: Measured button electrode response using a strip-line to simulate the beam. The inset shows a block diagram of the pre-amplifier circuit.

SyncLight Upgrades

Further remote controlled opto-mechanics are planned such as beam splitters which will allow for several optical beam lines to be served simultaneously at each station. This will also allow for minimal need to disturb the main camera for special studies. A multi-anode PMT in place of the camera is also being tested. Several vendors offer 8x8 detectors which could provide turn by turn images as well as single electron sensitivity.

Optical Stochastic Cooling

Optical stochastic cooling (OSC) extends the principle of stochastic cooling to optical frequencies and provides a means to manipulate an individual particle with its own radiation. As the bandwidth of the system controls the cooling rate, OSC has the potential for several orders of magnitude increase over conventional stochastic cooling. The basic principle is shown in Figure 19. For electrons in the IOTA ring, the OSC is expected to provide a factor of 20-40x damping rate when compared with the synchrotron radiation damping [9].

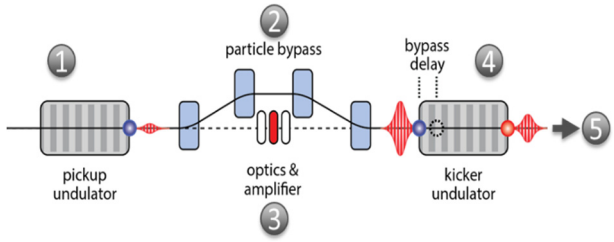

Figure 19: Schematic for the OSC experiment at IOTA.

Proton Injector

Research with high intensity proton beams will begin after the completion of proton source which was formerly used for the HINS test facility [10] and the corresponding injection line shown in Figure 20. The proton injector is expected to be completed 2020 with science program scheduled to begin in fiscal year 2021. The focus of the proton program will be on space-charge compensation and suppression of coherent instabilities. Once the proton source is ready, the IOTA ring will be able to accept either protons or electrons with some minimal reconfiguration. This provides some challenges for the diagnostics such as the BPMs. New instrumentation for beam profiles is also being investigated such as gas jet monitors [11].

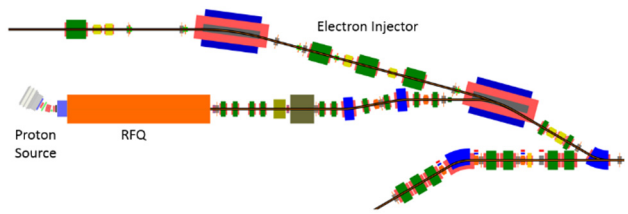

Figure 20: Layout for the proton injection line.

Electron Lens

An electron lens as shown in Figure 21 is currently under development and will be installed as part of the proton program [12]. The system will allow a wide range of non-linear studies by having a non-destructive and highly controllable field-forming current distribution overlap with circulating beam. In addition, the electron lens can also be used for space-charge compensation with electron beam and for electron cooling studies.

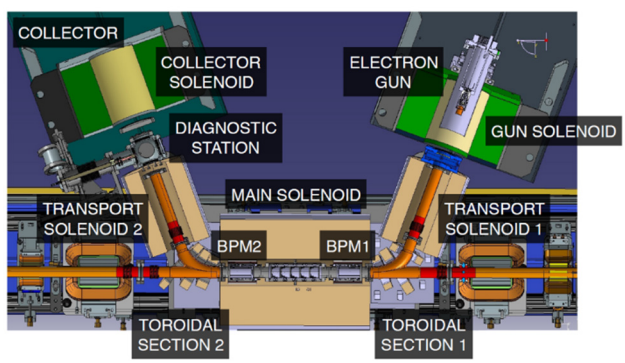

Figure 21: Layout for the electron lens at IOTA.

ISBN: 978-3-95450-204-2 ISSN: 2673-5350 doi:10.18429/JACoW-IBIC2019-MOBO02

SUMMARY

The first run was successfully concluded for the IOTA ring at Fermilab. This included initial commissioning of many components. Due to unforeseen issues, the commissioning took about a month longer than expected which limited the amount of time for the experimental program. Even so, the experimental program was also quite successful with most planed experiments able to collect data and achieve their goals as well as new experiments being designed and implemented during the course of the run. As a dedicated R&D facility, this model of commissioning new components and carrying out experiments in tandem will continue and is part of the benefit and price of a dedicated R&D facility. Work is underway to prepare for the next run to begin this fall.

ACKNOWLEDGEMENTS

The successful operation of the FAST facility and IOTA are the result of dedicated work by many people at Fermilab as well as other institutions and companies over many years. Thanks to all the participants who contributed to its success.

REFERENCES

[1] D. Broemmelsiek *et al*., "Record High-Gradient SRF Beam Acceleration at Fermilab", *New J. Phys.*, no.11, Nov. 2018. doi:10.1088/1367-2630/aaec57

[2] A. L. Romanov *et al*., "Commissioning and Operation of FAST Electron Linac at Fermilab", in *Proc. IPAC'18*, Vancouver, Canada, Apr-May 2018, pp. 4096-4099. doi:10.18429/JACoW-IPAC2018-THPMF024

[3] V. Danilov and S. Nagaitsev, "Nonlinear accelerator lattices with one and two analytic invariants" *Phys. Rev. ST Accel. Beams*, vol. 13, p. 084002, Aug. 2010

[4] S. Antipov *et al*., "IOTA (Integrable Optics Test Accelerator) facility and experimental beam physics program", *J. Instrum.* vol. 12, no. 03, T03002, 2017

[5] N. Kuklev *et al*., "Synchrotron Radiation Beam Diagnostics at IOTA – Commissioning Performance and Upgrade Efforts", in *Proc. IPAC'19*, Melbourne, Australia, May 2019. doi:10.18429/JACoW-IPAC2019-WEPGW103

[6] A. Reiter et al., "Comparison of beam position calculation methods for application in digital acquisition systems" *Nucl. Instrum. Meth.*, A890, pp. 18-27, 2018. doi:10.1016/j.nima.2018.02.046

[7] R. Barlow *et al*., "EMMA: The world's first non-scaling FFAG", *Nucl. Instrum. Meth.*, A624, pp. 1-19, 2010. doi:10.1016/ j.nima.2010.08.109

[8] A. L. Romanov *et al*., "Recent results and opportunities at the IOTA facility", presented at *NAPAC'19*, Lansing, Michigan, Sept 2019

[9] J. D. Jarvis *et al*., "Optical Stochastic Cooling Experiment at the Fermilab IOTA Ring", in *Proc. 61st ICFA & HB'18*, Daejeon, Korea, June 2018. doi:10.18429/JACoW-HB2018-TUP2WA01

[10] R. C. Webber and G. Apolinari., "Overview and Status Update of the Fermilab HINS Linac R&D Program", in *Proc. PAC'09*, Vancouver, Canada, May 2009

[11] S. Szustkowski *et al*., "Development of a Gas Sheet Beam Profile Monitor for IOTA", in *Proc. IPAC'18*, Vancouver, Canada, Apr-May 2018. doi:10.18429/JACoW-IPAC2018- WPAL065

[12] G. Stancari *et al*., "Electron Lenses and Cooling for the Fermilab Integrable Optics Test Accelerator", in *Proc. COOL'15*, Newport News, Virginia, Sep-Oct 2015